The 23 June 2020, Mw 7.4 La Crucecita, Oaxaca, Mexico earthquake and tsunami: A Rapid Response Field Survey during COVID-19 crisis

María-Teresa Ramírez-Herrera*, David Romero, Néstor Corona, Héctor Nava, Hamblet Torija, Felipe Hernández M.

* Corresponding author full address: Laboratorio de Tsunamis y Paleosismología, Instituto de Geografía, Universidad Nacional Autónoma de México. Av. Universidad 3000, UNAM, Coyocán, Ciudad de México, C.P.04510, tramirez@igg.unam.mx.

Abstract

The 23 June 2020 La Crucecita earthquake occurred at 10:29 hr on the coast of Oaxaca in a Mw 7.4 megathrust event at 22.6 km depth, and triggered a tsunami recorded at Huatulco and Salina Cruz tide gauge stations and a DART off the coast of Mexico. Immediately after the earthquake, a rapid response effort was coordinated by members of the Tsunami and Paleoseismology Laboratory UNAM, despite the challenges by the COVID-19 pandemic crisis, a post-earthquake and post-tsunami field survey went ahead 2 days after the event. We describe here details of the rapid response survey focusing on evidence of vertical coseismic deformation, tsunami, geologic effects, and lessons from working in the field during the COVID-19 crisis. We surveyed 44 km along the coast of Oaxaca focusing on preselected sites. Because of COVID-19 pandemic, some local communities enforced rules of confinement. We solved most of the challenges faced during this crisis by rapid networking with local organizations prior to surveying. We assessed coseismic uplift by means of mortality caused by vertical displacement of intertidal organisms and resurveying of bench marks, and measured tsunami runup using a laser ranger and GPS. Our results show coastal uplift of 0.53 m near the epicenter, decreasing farther away from it, and up to 0.8 m, the latest related to exposure of the coast. Our values of coastal uplift, ca. 0.53 m near the epicenter, fit well with 0.55 m of uplift reported by tide gauge data at Huatulco. Coastal uplift and low tide at the time of the event limited the tsunami inundation and runup on the Oaxaca coast. Nevertheless, we found tsunami inundation evidence at four confined coastal sites reaching a maximum runup of 1.5 m. The enclosed morphology of these sites determined higher runup and tsunami inundation . Local coastal morphology effects are not detected in tsunami models lacking detailed bathymetry and topography. This issue needs to be addressed during tsunami hazard assessments.

1. Introduction

23 June 2020 La Crucecita Earthquake and tsunami

The 23 June 2020 La Crucecita earthquake occurred at 10:29 hr (local time), at 15.784° N and 96.120° W, and ruptured an estimated 30 km by 20 km (USGS) segment of the Mexican subduction zone along the coast of Oaxaca in a Mw 7.4 megathrust event at 22.6 km deep (SSN, 2020), west of the intersection of the Tehuantepec ridge with the trench (Fig. 1). This earthquake triggered a tsunami recorded at Huatulco and Salina Cruz tide gauges (SMN, 2020), and a DART off the coast of Mexico (PTWC, 2020). A tsunami alert by the Pacific Tsunami Warning Center

(PTWC) was issued at 10:39 hrs. The earthquake left at least 10 people dead on the Oaxaca highlands and no tsunami damage was reported. Immediately after the earthquake, a rapid response effort was coordinated by members of the Tsunami and Paleoseismology Laboratory, Instituto de Geografía, UNAM and despite the challenges by the COVID-19 pandemic crisis, a post-earthquake and post-tsunami field survey went ahead 2 days after the event. We describe here details of the rapid response survey, challenges faced during a COVID-19 crisis, and results on measurements of coseismic deformation, tsunami runup observations, and other geologic effects generated by the earthquake.

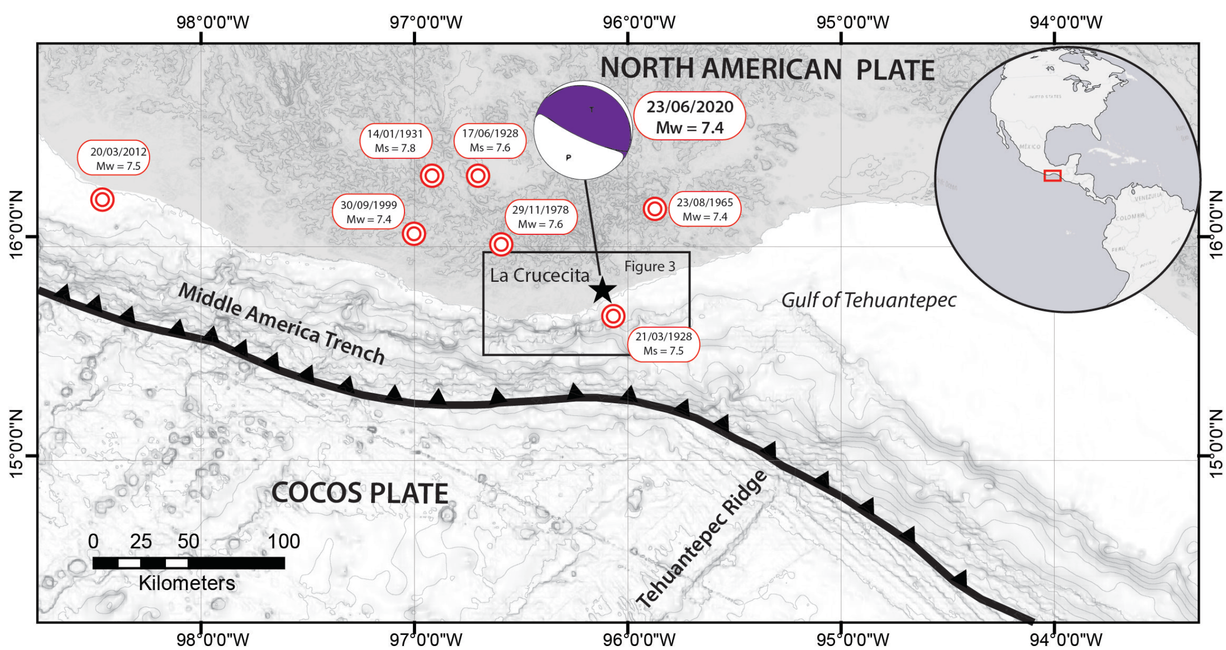

Figure 1. Tectonic and earthquakesetting. Red bullseye – Mw> 7 earthquakes in the Oaxaca region (SSM, 2020b);star – 23 June 2020 epicenter (SSM, 2020a); Moment tensor of the 23 June 2020 earthquake (USGS (2020).

Figure 1. Tectonic and earthquake setting. Red bullseye – Mw> 7 earthquakes in the Oaxaca region (SSM, 2020b); star – 23 June 2020 epicenter (SSM, 2020a); Moment tensor of the 23 June 2020 earthquake (USGS (2020).

Tectonic and earthquake setting

The 23 June 2020 La Crucecita earthquake nucleated at the Cocos-North America plate boundary (Fig. 1) with a Mw 7.4 (SSN, 2020a). Convergence rates in this sector of the Mexican subduction zone are near 70 mm/yr (DeMets et al, 2010). The megathrust event (strike= 266.8 , dip= 17.2, slip= 60.5) reached a maximum slip of 3.2 m slip (SSN, 2020a), although the USGS reported 7.5 m maximum slip (USGS, 2020). The Servicio Mareográfico Nacional (SMN, 2020) reported a +0.55 m land-level change recorded at the HUAT tide gauge. More than 7,000 aftershocks were recorded by July 14, 2020, the largest of which had a Mw 5.5 and occurred at 21:33 hr on 23 June 2020. Large earthquakes, Mw > 7 , are common in this region and several have been recorded during the last and this centuries (Kostoglodov and Ponce, 1994; Ramírez-Herrera et al., 1999; SSN, 2020b). Earthquakes of this magnitude have rupture areas of about 70 x 35 km (length x width) according to the USGS (2020), and earthquakes such as the Mw 6.4, the Puerto Angel earthquake of 1998 produced coastal uplift (Ramírez-Herrera and Zamorano, 2002).

Tsunami

The instrumental record indicates that the 1978 Mw 7.7 (Sanchez and Farreras, 1993) and the 2012 Mw 7.5 produced tsunamis (Ramírez- Herrera, personal comm.) (Fig. 1). However, historical events registered in archives indicate that great earthquakes and tsunamis have occurred in historical time and geological evidence of the 1787 and probable predecessor in 1537 have flooded the southwest coast of Mexico (Ramírez-Herrera et al., 2020). However, because of the short instrumental record, tsunami hazard has been minimized and incorrectly evaluated on the Pacific coast of México.

Coastal land level changes and mortality of intertidal organisms

Sudden coastal uplift has been documented using mortality of intertidal organisms and upper subtidal algae to estimate coseismic land-level changes particularly in subduction zones (e.g. Plafker, 1964; Johansen, 1971; Bodin And Klinger, 1986 ; Plafker and Ward, 1992; Pelletier et al, 2000; Ortlieb et al., 1996; Ramírez-Herrera and Zamorano, 2002; Lagabrielle et al., 2003; Farías et al., 2010; Melnick et al., 2012). Vertical zonation of intertidal species depends on factors associated with the tidal cycle (Lunning, 1990; Ortlieb et al. 1996).

Sudden uplift by earthquakes produces mortality among intertidal organisms, normally life dependent on the time they are exposed during low tides. Intertidal organisms mortality is commonly accompanied by whitening (bleaching) of the dead organism generating a white belt that differentiates clearly from the pinkish color of living organisms right below (Johansen, 1971; Ortlieb et al., 1996).

We used intertidal organisms to evaluate coseismic coastal uplift associated with the 23 June 2020 Oaxaca earthquake using coralline algae and invertebrate species living at intertidal and upper subtidal, and in few cases the supralitoral, marine habitats (Ramírez-Herrera & Zamorano 2002, Castilla et al. 2010). The intertidal habitat is between the highest and the lowest levels of the tidal range. The biological communities in this habitat may be adapted to be submerged and emerged periodically due the influence of the daily tides. The upper subtidal habitat begins below the lowest level of the intertidal range, and the species inhabiting there are permanently submerged. Supralittoral habitat is submerged only occasionally during the highest spring tides and mainly is influenced by the sea waves and the marine breezes (Tait & Diper 1998).

Rapid response

The 23 June 2020 earthquake and tsunami occurred during the COVID-19 pandemic crisis, despite this we coordinated a rapid response effort and a post-earthquake and post-tsunami field survey went ahead 2 days after the event. We contacted a local network of people in positions that allowed us rapid access to surveyed sites before the evidence was obliterated by rain and/or human activity.

2. Field Survey

Two days after the 2020 Oaxaca earthquake, we started a five-day survey, despite challenges and restrictions imposed by the COVID-19 pandemic, which were related to safe flight travel, confinement, closed hotels and restaurants, to rapidly measure tsunami runup and coastal coseismic deformation, marked by the elevation of bleached intertidal organism belts, and surveying of benchmarks by SMN. We focused at the Huatulco bays region on 15 locations along 44 km of the coast (Fig. 1). The width of bleached intertidal organisms and upper subtidal algae belt, marked by the top and base of the belt, was measured directly on the bleached belt using a metric tape on exposed to waves rocky outcrops and on exposed coral reefs, and only few measurements were made with laser rangefinder when sites were not reachable. We measured tsunami runup by means of marks above the high tide level using a laser rangefinder. Laser rangefinder precision on short distances, < 100 m, is < 5 cm, and measures directly on the exposed rock with tape had less than 0.5 cm error. We photographed all measured sites and located them with a GPS recording time to assess tide levels at the time of measurement. We also surveyed coral reefs using a drone TBS Discovery to map the bleached coral reef areas.

Tide gauge data from Servicio Mareográfico Nacional (SMN) at Huatulco station (see Table S1 of Supplemental material) were used to assess the living position and mortality of intertidal organisms used in this study to estimate coastal uplift.

3. Observations and results

Bleaching or mortality of intertidal organisms

We identified several species of bleaching organisms and their taxonomy as well as their habitat summarized in Table S2 of the Supplemental material. We also use corals from coral reefs that showed signs of bleaching and emergence. Based on collected samples of organisms and photographs taken in the field, the taxonomic identity of all species were verified with literature available for the area and the World Register of Marine Species (WORMS). Their taxonomy is also summarized in Table S2 and Figure S1 of Supplemental material. In summary, the organism identified and used in this study are: a) green algae *Ulva prolifera*, b) gastropod *Nerita* *scabricosta*, c) gastropod *Lottia pediculus*, d) bivalve *Crassostrea corteziensis*, e) vermetid *Petaloconchus complicatus*, f) polychaete *Salmacina tribranchiata*, g) crustacean *Amphibalanus eburneus*, h) bivalve *Chama coralloides*, i) crustacean *Megabalanus coccopoma*, j) coralline algae *Lithophyllum* sp., k) stony coral *Pocillopora verrucosa* and l) stony coral *Pocillopora damicornis*. Vertical zonation of the organisms used in this study is shown in Figure 2 on and Table S2 of Supplemental material. Mean tidal range is 0.89 m, extreme tidal range is 1.02 m, and maximum extreme tidal range is 1.02 m at this stretch of the Oaxaca coast (Grivel & Grivel, 1993).

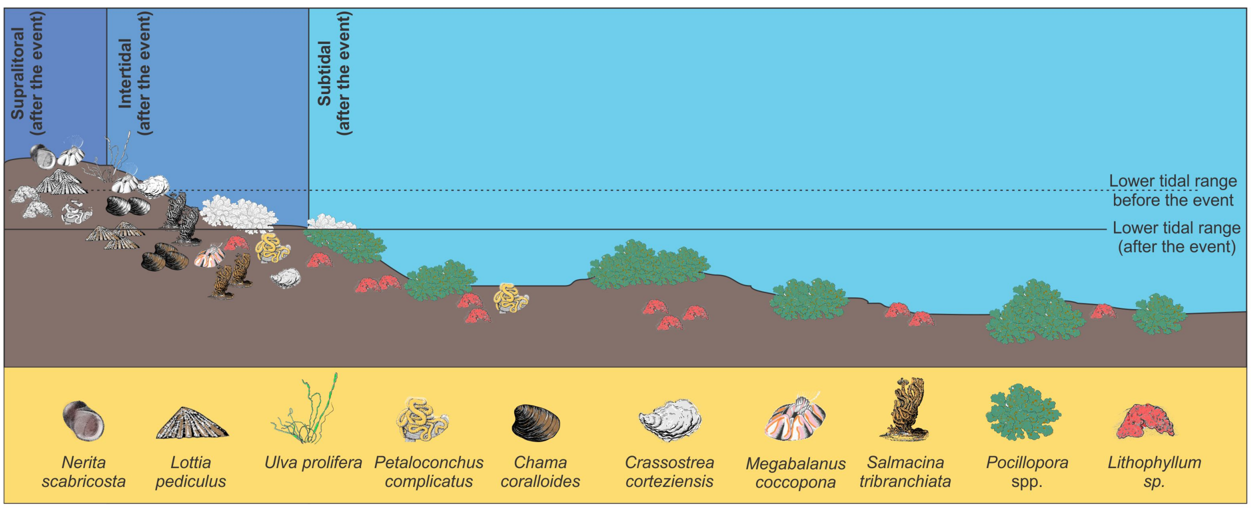

Figure 2. Vertical zonation of the organisms used in this study.

Figure 2. Vertical zonation of the organisms used in this study

Coastal Uplift

We measured the bleaching belt of organisms indicative of mortality at 15 locations along the Oaxaca coast (Fig. 3). We collected several measurements at different sites, where possible more than one measurement was registered at each location to have a statistically representative value. Only four sites showed values that did not satisfy the quality criteria (Ortlieb et al., 1996). These values were measured on sites on enclosed tide pools; two high values were measured in an estuary, and one site showed exposed corals difficult to measure from a far distance.

Our results on measuring the bleaching belt of intertidal organisms indicates that coastal uplift produced by the Mw 7.5 Huatulco earthquake extended along 44 km between San Isidro west of the epicenter, and Barra de la Cruz east of the epicenter (Fig. 3). The further west and east of the epicenter showed low to none evidence of intertidal organisms mortality. The coastal stretch at Playa El Violin, Playa La Yerbabuena, Playa Pescadores-Quinta Real, Fonatur dock, and Playa Pescadores- Santa Cruz showed clear evidence of widespread intertidal organism bleaching belt (OBB). The width of OBB ranged from 0.1 up to 0.8 m along the surveyed area. However, the largest values do not fit the criteria for assessing coastal uplift and are reflecting amplification of the OBB by local features such as coastal morphology (intertidal pools, estuaries, wave splash and far distance features). Those values are excluded from the final estimate of coastal uplift.

The OBB width at FONATUR dock ranged from 0.4 to 0.54 m, and a mean of 0.47 m (Fig. 3 and Fig. 4). At Playa Pescadores-Santa Cruz the OBB width values ranged from 0.5 to 0.56 m with a mean of 0.535 m. We consider these values to be representative of the uplift in this area. At Marina Chahue values range from 0.2 to 0.4, mean value is 0.28 m. We excluded the largest value of 0.8 m because it reflected the amplification of the local intertidal pool. At Playa Pescadores-Quinta Real we measured a relatively high value of 0.6 m. This is caused by the effect of a narrow channel fenced by two breakwater structures on both sides. Further to the NE, at la Bocana, the mean value of OBB width was 0.37 m. At Zimatan-Laguna Las Garzas beach, values range from 0.2 to 0.3 m., which reflects the decrease in uplift away from the area of the epicenter. At Zimatan-Laguna Las Garzas river mouth, values were high, mean value 0.77 m. This site does not reflect the real deformation because the vertical distribution of intertidal organisms here is influenced by specific characteristics of the location (Ortlieb et al, 1996). At Barra de La Cruz, we were not granted access to the beach due to COVID-19 lockdown measures taken by the locals. To the west of the epicenter, at Playa Yerbabuena (SEMAR) values ranged from 0.2 to 0.53 m, with a mean value of 0.32 m. Playa Violin showed OBB width ranged from 0.29 to 0.57 m, mean value is 0.42 m (Fig. 3 and Fig. 4). At Bahía El Órgano, representative values ranged from 0.2 to 0.4 m. We did not include an extremely high value of 0.8 m produced by the local site effect (an enclosed tidal pool). Playa Riscalillo showed coral reef bleached width ranging between 0.10 to 0.20 m. San Agustin bay also showed coral reef exposed above mean sea level, however the distance to the reef precluded us from taking a precise measure, thus we excluded the 0.70 m value that is not representative. At Playa del Amor values ranged from 0.10 to 0.20 m which are consistent with an expected decrease of OBB width away from the epicenter. The furthest west location, at San Isidro evidence was scarce and the belt measured at the mouth of an estuary showed values in between 0.15 and 0.20 m, reflecting site increment effects. The latest suggests that uplift here was minimal, perhaps less than a few centimeters. We did not expect to find evidence further to the west since last site only showed patchy evidence of OBB.

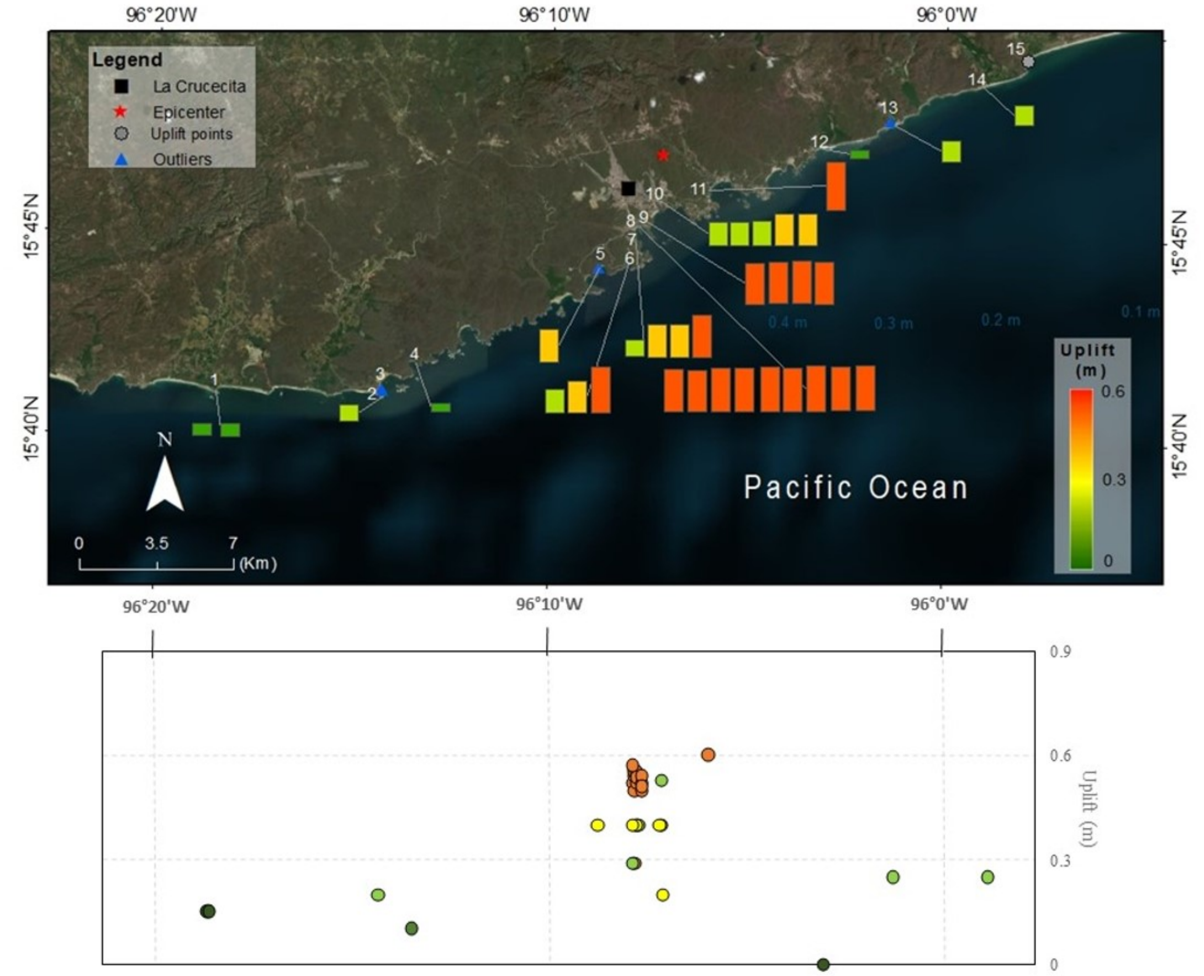

Figure 3. Coseismic uplift generated by the La Crucecita Mw 7.4, 23 June 2020, earthquake. Bars indicate the width (m) of the organisms bleached belt (OBB) at 15 locations along 44 km of coastal stretch: 1. San Isidro, 2. Playa del Amor, 3. San Agustín, 4. Bahía Riscalillo, 5. Playa el Órgano, 6. Playa el Violín, 7. Playa Yerbabuena – SEMAR, 8. Playa Pescadores, 9.Fonatur dock, 10. Marina Chahué, 11. Playa Pescadores – Quinta Real, 12. La Bocana Río Copalita, 13. Río Zimatán, 14. Zimatán – Laguna las Garzas, 15. Barra de la Cruz. Blue triangles – sites with values > 0.5 m. Please see the text for explanation.

Figure 3. Coseismic uplift generated by the La Crucecita Mw 7.4, 23 June 2020, earthquake. Bars indicate the width (m) of the organisms bleached belt (OBB) at 15 locations along 44 km of coastal stretch: 1. San Isidro, 2. Playa del Amor, 3. San Agustín, 4. Bahía Riscalillo, 5. Playa el Órgano, 6. Playa el Violín, 7. Playa Yerbabuena – SEMAR, 8. Playa Pescadores, 9. Fonatur dock, 10. Marina Chahué, 11. Playa Pescadores – Quinta Real, 12. La Bocana Río Copalita, 13. Río Zimatán, 14. Zimatán – Laguna las Garzas, 15. Barra de la Cruz. Blue triangles – sites with values > 0.5 m. Please see the text for explanation.

Figure 3 summarizes the distribution and amount of coseismic uplift estimated from OBB. We have used all values and mean values to graphically represent the width of the OBB. These values are estimates of the land level change, i.e. coseismic uplift by the 23 June 2020 earthquake. We use only values that best represent the uplift and excluded values from locations that were influenced by site effects. The maximum estimated uplift was identified at Playa Pescadores- Santa Cruz, FONATUR duck, Playa Pescadores-Quinta Real, and Playa El Violin. From this area on, to the west and northeast farther away from the earthquake epicenter, values of uplift tend to decrease. Uplift represented by mortality of intertidal organisms extended about 40 km along the coast. We are not sure about the extent of uplift further NE since we were prevented access to locations from Barra de La Cruz on, however we already observed a decrease in uplift at the nearest location. The general pattern of coseismic uplift indicated by the OBB width suggests greater land vertical motion closer to the epicenter.

Figure 4. Mortality of intertidal organisms caused by sudden land uplift shown by a bleaching belt of intertidal organisms. UL = Upper limit and LL Lower limit of organism bleached belt. a) La Bocana Río Copalita , b) San Isidro, c) Bahía Riscalillo – aerial view of patches of bleached coral reef, d) Marina Chahué, e) Playa el Violín, f) Bleached coral reef at Bahía Riscalillo g) Playa Yerbabuena – SEMAR – bleached coral, h) Playa Pescadores, i). Detail of bleached belt at Playa Pescadores.

Figure 4. Mortality of intertidal organisms caused by sudden land uplift shown by a bleaching belt of intertidal organisms. UL = Upper limit and LL Lower limit of organism bleached belt. a) La Bocana Río Copalita , b) San Isidro, c) Bahía Riscalillo – aerial view of patches of bleached coral reef, d) Marina Chahué, e) Playa el Violín, f) Bleached coral reef at Bahía Riscalillo g) Playa Yerbabuena – SEMAR – bleached coral, h) Playa Pescadores, i). Detail of bleached belt at Playa Pescadores.

We measured the elevation of two benchmarks set by the SMN to have a different data parameter and being able to compare and determine with more parameters land-level changes. The first bench mark (BN20HUA01) is located at the Fonatur dock next to the tide gauge and the second bench at the park kiosk (BN20HUA02). Bench mark BN20HUA01 showed 0.528 m uplift and BN20HUA02 experienced 0.491 m uplift after the 23 June 2020 earthquake.

Tsunami

A tsunami was generated by the Mw 7.4 La Crucecita earthquake. The earthquake occurred at 10:29 hr local time. The SMN Huatulco tide gauge registered a maximum tsunami amplitude of 0.61 m at 13:12 hr local time, and at Salina Cruz tide gauge station with a maximum amplitude of 1.394 m at 12:34 hr local time (Fig. S2 Supplemental material). According to the registered tide gauge data, the sea started retreating at 10:30 hr reaching a maximum retreat of -1.273 m at 10:36 hr. TheSMN Huatulco interpretation suggests that the tsunami initiated at 11:12 hr reaching a maximum amplitude of 0.61 m at 13:12 hr, and ending at 18:06 hr (Fig. S2 Supplemental material)

However, we observed several videos recorded by static camera devices at the FONATUR dock and estimated that the sea started to retreat approximately 5 to 7 minutes after the earthquake (the retreat could have started earlier since power went off and 5 minutes of record were lost), with turbulence and sediment in suspension, and reached the lowest level 11 minutes after the earthquake. The sea apparently made a return, with relative strong energy and speed, 13 minutes after the earthquake, i.e. at approximately between 10:43 or 10:45 hr local time. At 10:47 again the sea retreated and reached a maximum height by 10:48 hr to again reach an apparent lower level than the one the sea showed before the earthquake.

According to social media and witnesses reports, the sea retreated almost immediately after the earthquake but did not cause extensive inundation nor damage was reported in coastal cities. Witnesses reported sea return but emphasized it never reached the sea level previous to the earthquake. After the earthquake some coastal residents started a timely evacuation to higher ground after seeing the sea retreat, however not all coastal residents evacuated. No damage nor deaths were reported due to the tsunami. The Mexican Tsunami Warning Center (CAT – Centro de Alertas de Tsunami) issued a tsunami alert, however none of the coastal residents we interviewed were aware of the tsunami warning other than the earthquake itself.

Tsunami marks left on the shore were scarce on the surveyed sites. We expected to find only a few marks after looking at tide gauge data reports of the 23 June 2020 tsunami on Huatulco and Salina Cruz stations, also because at the time of earthquake and tsunami the tide level was low (-0.582 m), and as explained above we observed a bleaching belt of intertidal organisms indicative of coastal uplift. However, we located sand and cobbles beyond high tide mark on boat ramps, organic debris (broken coral) higher than the highest tide mark on a beach, and other organic debris, at four sites along 44 km of the surveyed coast. At Playa El Violin we found a line of broken corals from a local coral reef located higher than the highest tide mark, indicative of tsunami runup ~ 0.9 m. This narrow and confined bay faces to the SW (Fig. 5). The second site at Marina Chahue, with a very narrow entrance to the Marina (Fig. 5), showed a tsunami mark made of sand and cobbles on a concrete ramp next to fuel pumps, and the measured runup was ~1.07 to 1.37 m. Playa Pescadores (Quinta Real) is an extremely narrow channel facing SE, confined by groins that might have increased the tsunami runup up to ~1.57 m. La Yerbabuena beach at the boat ramp, confined by a dock and a cliff, also showed a tsunami mark made of sand and cobbles with a runup of 0.99 m (Fig. 5). All these sites have in common being narrow and confined. We explained the absence of tsunami marks by: 1) low tide at the time of tsunami and 2) land uplift of this portion of the coast caused by the earthquake, that decreased the size of the tsunami. The few tsunami marks left on the shore can be explained by the local morphology of these sites: very narrow confined channels and likely the bathymetry of a narrow entrance bay. These local effects cannot be envisaged in tsunami models due to the gross topography bathymetry used in modeling, and this is an issue that requires to be addressed when using modeling in tsunami hazard assessment.

Figure 5. Tsunami runup marked by debris at four locations along the study area. a) El Violín Beach, b) Marina Chahué, c) Playa Yerbabuena – SEMAR.

Figure 5. Tsunami runup marked by debris at four locations along the study area. a) El Violín Beach, b) Marina Chahué, c) Playa Yerbabuena – SEMAR.

Other Geologic effects (liquefaction, fissures, landslides)

We observed near the coast several geologic effects associated with the Mw 7.4 earthquake´s ground shaking, with PGA 20% g and PGV 41.4 cm/s, intensity VIII near the epicenter (USGS, 2020) (Fig. 1). Rockfalls and landslides were common along coastal highways and on some slopes, however their size was relatively small. Lateral spreading, fissures on the ground and beaches were common. Liquefaction (sand boils) was focused near estuaries, river mouths, and lagoons (Fig. 6). Most of the landslides were reported on the Oaxaca highlands and these were not included in the scope of this survey. It is worth mentioning that the current rainy season at the time of the earthquake in Oaxaca, Mexico, most probably increased slope failures.

Figure 6. Other Geologic effects: liquefaction, fissures, landslides caused by La crucecita earthquake of 23 June 2020. a) Playa Pescadores – Quinta Real, b), c) and g) Zimatán-Laguna las Garzas, d) La Bocana Río Copalita, e), f) Boulevard Chahué.

Figure 6. Other Geologic effects: liquefaction, fissures, landslides caused by La crucecita earthquake of 23 June 2020. a) Playa Pescadores – Quinta Real, b), c) y g) Zimatán-Laguna las Garzas, d) La Bocana Río Copalita, e), f) Boulevar Chahué.

Buildings along the coast apparently had very few damage. Although beyond the scope of this survey, we noticed mainly a few 3 to 4-store buildings that showed structural damage. Most of the hotels and houses close to the beach responded well with minor damage (broken roof tiles).

Surveying during COVID-19 crisis

Field survey was carried out in the state of Oaxaca during the COVID-19 pandemic crisis. Santa María Huatulco was selected as the operation center, since this was the area of the La Crucecita earthquake epicenter. On the arrival day, the epidemiological panorama of the coastal region showed 170 COVID-19 active cases, and at Santa María Huatulco only 7 COVID-19 cases. We followed all recommendations regarding prevention during the course of the post-earthquake and tsunami survey: all the participants involved wore masks, the use of alcohol gel, frequent hand washing and keeping a 1.5 m distance. Only one vehicle was used during the survey, which was washed and disinfected every day, the interaction with people during field work was always respecting a safe distance and the use of masks, in addition to the permanent vigilance for the appearance of any symptoms by the team members (Fig. 7).

Figure 7. Surveying during COVID-19 crisis. a) Arrival at Huatulco airport and reception by the Bomberos de Oaxaca (Oaxaca Firemen). b) SEMAR (Mexican Navy) vessel used to reach inaccessible by land coastal locations. c) Instructions and discussion with SEMAR members keeping a safe distance and wearing masks. d) Sign at Barra de La Cruz indicating restricted access to the town due to COVID-19 confinement.

Figure 7. Surveying during COVID-19 crisis. A) Arrival at Huatulco airport and reception by the Bomberos de Oaxaca (Oaxaca Firemen). b) SEMAR (Mexican Navy) vessel used to reach inaccessible by land coastal locations. c) Instructions and discussion with SEMAR members keeping a safe distance and wearing masks. d) Sign at Barra de La Cruz indicating restricted access to the town due to COVID-19 confinement.

We faced a few challenges and restrictions imposed by the COVID-19 pandemic. Prior to traveling we contacted our local network in Huatulco, Oaxaca, to rapidly get access to sites along the coast. Traveling to the coast in a rapid way required flying in a packed airplane with no empty seats in between passengers. Due to the confinement in some towns most hotels and restaurants were closed, however we had the support of the La Crucecita, Huatulco, Firemen

(Bomberos de Oaxaca), and FONATUR (the Federal office for tourist affairs) who kindly arranged for us to use a truck and hotel reservations during the survey. To get rapid access to less accessible sites, the Navy local office aided in using a Navy boat (Fig. 7). All of this was arranged previous to arrival by our local contact with Oaxaca Firemen. It is therefore very important to have a good network and work with locals in times of crisis for a rapid evaluation of earthquake and tsunami effects.

During the survey, we always respected the local practices and actions of containment because of the pandemic. We first talked with the local authorities at checkpoints to ask for access, as it was the case in the community of La Bocana and Copalita. However, we could not have access to some places, such as the community of Barra de La Cruz where access to anyone outside the community was prohibited (Figure 7). We solved this situation by visiting the nearest possible site to make observations.

Summary and Discussion

The 23 June 2020 La Crucecita earthquake produced coastal uplift recorded by the extent of mortality of intertidal organisms caused by sudden vertical motions. A white belt of dead organisms appeared at several sites along the coast and was already visible by the second day after the earthquake. The width of this belt varied along the coast, generally showing higher values near the epicenter and decreasing further away. Evidence of coastal deformation was observed between San Isidro and Zimatan (Fig. 3), that we considered the along-strike extent of the 23 June 2020 La Crucecita earthquake rupture of ca. 40 km. Our results based on the interpretation of most representative values that fulfilled the criteria explained above, show coastal coseismic uplift of 0.53 m near the epicenter and farther away decreasing to 0.10 m. The bleached belt of intertidal organisms is a reliable estimate of the uplift produced by the 23 June 20202 La Crucecita earthquake. Other phenomena such as extremely low tide and El Niño events cannot explain the mortality of intertidal organisms since, firstly we surveyed sites that had experienced low tide sequences and 2020 had no El Niño event on the coast of México. Furthermore, fishermen and locals pointed to the "no return of the sea to its normal level after the earthquake", i.e. coastal land level change, and to the mortality of coral reefs and other intertidal organisms. Furthermore, we corroborated our results with measurements of two geodetic SMN benchmarks at Santa Maria Huatulco near la Crucecita. Our results using benchmarks height measurements confirm coastal uplift of 0.528 m on the coast and 0.491 m slightly inland (Fig. 3). Also, we used the SNM tide gauge data (Fig. S1 of Supplemental material) and SNM report that indicates coastal uplift of 0.55 m. Therefore the observed bleached belt reliably represents coseismic uplift produced by the 23 June 2020 La Crucecita earthquake. We suggest that the use of organisms sudden mortality aids in a rapid survey of earthquake deformation along the coast.

Tsunami evidence was scarce and our measurements of tsunami runoff on the surveyed coastal stretch showed 0.9 m and a maximum runoff of 1.5 m at four confined coastal sites. The scarcity of tsunami evidence can be explained by several factors. Firstly, it was raining during and the night after the event, thus evidence such as debris are not perennial and could be easily washed away by rain. Secondly, the tide level at the tsunami arrival was low (-0.58 m), which also contributed limited tsunami inundation and runoff at the coast. Finally, coastal uplift of ca. 0.53 to 0.10 m, also limited tsunami inundation and runoff. Despite all of the explained above, we observed evidence at four coastal sites with confined coastal morphology. Tide gauge records, testimonies by locals, and video recordings also support evidence of the sea retreat and energetic sea return, even if with relatively low tsunami heights, a few minutes (~5 to 7 minutes) after the earthquake.

Thus, it is important to remember and emphasize that historical and prehistorical earthquakes produced great tsunamis on the Mexican Pacific coast, such as the 1787 event and the possible predecessor of 1537 (Ramírez-Herrera et al., 2020). Instrumental data unfortunately do not capture in their short record (ca. 100 years) in Mexico all tsunamigenic events, nor all earthquakes produced coastal uplift on the Pacific coast of Mexico. For instance, the 1995 Mw 8.0 Colima-Jalisco earthquake produced coastal subsidence and a significant tsunami with run-up height of 5.1 m (e.g. Pacheco et al., 1997; Borrero et al., 1997; Trejo-Gómez et al., 2015). Even when earthquakes produced coastal uplift, as it happened during the 19 September 1985 Mw 8.1 (Bodin and Klinger, 1986) and 20 September 1985 Mw7.5 earthquakes, two tsunamis flooded the coast of Michoacan and Guerrero, Mexico (Sanchez and Farreras, 1993) leaving geologic evidence (Ramírez-Herrera et al., 2012). It is also possible that shallow events near the trench might cause coastal subsidence and large tsunamis such as the 1787 event (Ramírez-Herrera et al., 2020) and the more recent 1995 Mw 8.0 Colima-Jalisco earthquake (Pacheco et al., 1997; Hjörleifsdóttir et al., 2018). Tsunami modeling exercises may aid in estimating tsunami amplitudes, however due to the lack of detailed bathymetry and topography, local coastal morphology effects are missed in models. Thus an effort should be made to produce bathymetric data near the coast to have reliable tsunami models. This and tsunami education programs are of most importance in tsunami hazard prevention to create tsunami resilient coastal communities.

Finally, our lesson from working during the Covid-19 pandemic crisis is that it is crucial to have a local network of collaborators who facilitate a rapid response during post-earthquake and tsunami surveys by aiding in getting access to localities and sites affected by this phenomena, assists in logistics, help in understanding and respecting local practices by communities that in turn cooperate in describing these phenomena.

Data and Resources

Supplemental material includes Table S1 presenting tide gauge data from Servicio Mareográfico Nacional (SMN) at Huatulco station. Data were used to assess living position and mortality of intertidal organisms.

Table S2 provides data on the taxonomic identity and vertical zonation of organisms used in this study.

Figure S1 includes details, taxonomy, and photographs of the organisms used in this study. Figure S2 shows the Huatulco tide gauge data interpretation of land-level vertical displacement and tsunami amplitude after the 23 June 2020 earthquake.

Acknowledgments

This work was supported by Instituto de Geografía, Universidad Nacional Autónoma de México and CONACYT-SEP 284365 granted to Ramírez-Herrera. We thank the following people and

Institutions for logistic help during the survey: Bomberos Oaxaca - Lic. Manuel A. Maza Sánchez; Secretaria de Marina - Sector Naval Huatulco- Contralmirante CGDEM Procoro Juan Trinidad García and Capitán Juan Solís Guillén, Secretaría de Seguridad Pública- Lic. Raul Ernesto Salcedo Rosales; Secretaria de Turismo - Delegación Regional Huatulco - Lic. Raúl Sinobas Solís, Fonatur - Delegación regional CIP Huatulco - Ing. Ramón Sinobas Solís, Capitanía del Muelle de Cruceros – Cap. Ángulo, FONATUR – Mario Harrigan. Víctor Vargas helped with figure drafting. Diego Melgar shared preliminary slip, vertical deformation, and tsunami amplitude models. We thank the coastal communities of Oaxaca visited during this post-earthquake and post-tsunami field survey for kindly giving access, sharing their memories and videos of the events.

References

Bodin, P., & Klinger, T. (1986). *Coastal uplift and mortality of intertidal organisms caused by the September 1985 Mexico earthquakes*. Science, 233, 1071–1073.

Borrero, J., Titov V., Ortiz M., , Synolakis C. (1997). Mexican Earthquake Generates Tsunami, New Data, and Unusual Photos. Earth in Space, vol. 9, no. 7, p. 5-8, 1997 American Geophysical Union. Retrieved July 21, 2020 from http://www.agu.org/sci_soc/eisborerro.html

Castilla, J. C., Manríquez, P. H., & Camaño, A. (2010). Effects of rocky shore coseismic uplift and the 2010 Chilean mega-earthquake on intertidal biomarker species. Marine Ecology Progress Series, 418, 17-23.

DeMets, C., Gordon, R. G., & Argus, D. F. (2010). Geologically current plate motions. *Geophysical Journal International*, *181*(1), 1–80.

Farías, M., Vargas, G., Tassara, A., Carretier, S., Baize, S., Melnick, D., & Bataille, K. (2010). Land-level changes produced by the 2010 Mw8. 8 Chile earthquake. *Science*, *329*, 916.

Grivel, P. F., & Grivel, F. V. (1993). Tablas de Predicción de mareas 1993. Puertos del Pacífico. *Servicio Mareografico Nacional. UNAM*, 115.

Hjörleifsdóttir V. Sánchez Reyes H. S. Ruiz Angulo A. Ramírez-Herrera M. T. Castillo-Aja R. Singh S. K., and Ji C. 2018. Was the October 9th 1995 Mw 8 Jalisco, Mexico earthquake a near trench event? J. Geophys. Res. doi: https://doi-org.pbidi.unam.mx:2443/10.1029/2017JB014899.

Johansen, H. W. (1971). Effects of elevation changes on benthic algae in Prince William Sound. *In :The Great Alaska Earthquake of 1964*, *Washington*, *D.C.: National Academy of Sciences*, p.35-68.

Kostoglodov, V., & Ponce, L. (1994). Relationship between subduction and seismicity in the Mexican part of the Middle America trench. *Journal of Geophysical Research*, *99*, 729–742.

Lagabrielle, Y., Pelletier, B., Cabioch, G., Régnier, M., & Calmant, S. (2003). Coseismic and long-term vertical displacement due to back arc shortening, central Vanuatu: Offshore and onshore data following the Mw 7.5, 26 November 1999 Ambrym earthquake. *Journal of Geophysical Research*, *108*, 2519.

Luning, K. S. (1990). *Their environment, Biogeography and Ecophysiology*. New York: John Wiley & Sons, Inc. 527p.

Melnick, D., Cisternas, M., Moreno, M., & Norambuena, R. (2012). Estimating coseismic coastal uplift with an intertidal mussel: calibration for the 2010 Maule Chile earthquake (Mw= 8.8). *Quaternary Science Reviews*, *42*, 29–42, ISSN 0277-3791. https://doi.org/10.1016/j.quascirev.2012.03.012

Ortlieb, L., Barrientos, S., & Guzman, N. (1996). Coseismic coastal uplift and coralline algae record in northern Chile: the 1995 Antofagasta earthquake case. *Quaternary Science Reviews*, *15*, 949–960.

Pacheco, J., Singh, S. K., Domínguez, J., Hurtado, A., Quintanar, L., Jiménez, Z., Yamamoto, J., Gutiérrez, C., Santoyo, M., & Bandy, W. (1997). The October 9, 1995 Colima-Jalisco, Mexico earthquake (Mw 8): An aftershock study and a comparison of this earthquake with those of 1932. *Geophysical Research Letters*, *24*, 2223–2226.

Pacific Tsunami Warning Center. (2020). *ITIC Tsunami Bulletin Board Tsunami, NWs Pacific Tsunami Warning Center Bulletin Jun 23 2020, NOAA*. Accessed 23 June 2020.

Pelletier, B., Régnier, M., Calmant, S., Pillet, R., Cabioch, G., Lagabrielle, Y., Bore, J.-M., Caminade, J.-P., Lebellegard, P., & Cristopher, I. (2000). Le séisme d'Ambrym–Pentecôte (Vanuatu) du 26 novembre 1999 (Mw: 7, 5): données préliminaires sur la séismicité, le tsunami et les déplacements associés. *Comptes Rendus de l'Académie Des Sciences-s-Series IIA-e-Sciences de 10 Terre et Des Planetes*, *331*(1), 21–28.

Plafker, G. (1964). Tectonic deformation associated with the 1964 Alaska earthquake. *Science*, *148*(3678), pp.1675-1687.

Plafker, G., & Ward, S. N. (1992). Backarc thrust faulting and tectonic uplift along the Caribbean Sea Coast during the April 22, 1991 Costa Rica earthquake. *Tectonics*, *11*, 709–718.

Ramírez-Herrera, M.-T., Corona, N., Cerny, J., Castillo-Aja, R., Melgar, D., Lagos, M., Goguitchaichvili, A., Machain, M. L., Vazquez-Caamal, M. L., Ortuño, M., Caballero, M., Solano-Hernandez, E., & Ruiz-Fernández, A. (2020). Sand deposits reveal great earthquakes and tsunamis at Mexican Pacific Coast. *Scientific Reports*, *10*, 11452. https://doi.org/10.1038/s41598-020-68237-2

Ramirez-Herrera, M.-T., Kostoglodov, V., Summerfield, M. A., Urrutia-Fucugauchi, J., & Zamorano, J. J. (1999). A reconnaissance study of the morphotectonics of the Mexican subduction zone. *ZEITSCHRIFT FUR GEOMORPHOLOGIE SUPPLEMENTBAND*, 207–226.

Ramírez-Herrera, M.-T., Lagos, M., Hutchinson, I., Kostoglodov, V., Machain, M. L., Caballero, M., Goguitchaichvili, A., Aguilar, B., Chagué-Goff, C., Goff, J., Ruiz-Fernández, A., Ortiz, M., Nava, H., Bautista, F., Lopez, G. ., & Quintana, P. (2012). Extreme wave deposits on the Pacific coast of Mexico: Tsunamis or storms?—A multi-proxy approach. *Geomorphology*, *139*, p.360-371. https://doi.org/10.1016/j.geomorph.2011.11.002

Ramirez-Herrera, M.-T., & Orozco, J. J. Z. (2002). Coastal uplift and mortality of coralline algae caused by a 6.3 Mw earthquake, Oaxaca, Mexico. *Journal of Coastal Research*, *18*, 75–81.

Sánchez Devora, A. J., & Farreras Sanz, S. (1993). *Catalog of tsunamis on the western coast of Mexico*. *Rep SE-50.*(World Data Center A for Solid Earth Geophysics, NOAA, National Geophysical Data Center, Boulder, Colorado, 1993).

Servicio Mareográfico Nacional, 2020. Reporte del tsunami producido por el sismo de magnitud 7.5 ocurrido el día 23 de junio de 2020 al sureste de Crucecita, Oaxaca. UNAM, México http://www.mareografico.unam.mx/portal/docu/Pdfs/Reporte_Servicio_Mareografico_23_junio_2020.pdf

Servicio Sismológico Nacional (SSN) (2020a) Reporte Especial - Sismo del 23 de Junio de 2020, Costa de Oaxaca (M 7.5). IGEF - UNAM, México. (http://www.ssn.unam.mx/sismicidad/reportes-especiales/2020/SSNMX_rep_esp_20200623_Oaxaca-Costa_M75.pdf)

Servicio Sismológico Nacional (SSN). (2020b). *Catálogo de Sismos.* http://www2.ssn.unam.mx:8080/catalogo/ (Last Accessed June 25, 2020).

Tait, R. V., & Dipper, F. (1998). *Elements of marine ecology*. Butterworth-Heinemann.

Trejo-Gómez, E., Ortiz, M., & Núñez-Cornú, F. J. (2015). Source Model of the October 9, 1995 Jalisco-Colima Tsunami as constrained by field survey reports, and on the numerical simulation of the tsunami. *Geofísica Internacional*, *54*(2), 149–159.

USGS. (2020). *M 7.4 - 9 km SE of Santa María Xadani, Mexico*. https://earthquake.usgs.gov/earthquakes/eventpage/us6000ah9t/ground-failure/summary

Full mailing address for each author

María Teresa Ramírez-Herrera, Laboratorio de Tsunamis y Paleosismología, Instituto de Geografía, Universidad Nacional Autónoma de México. Av. Universidad 3000, UNAM, Coyocán, Ciudad de México, C.P.04510, tramirez@igg.unam.mx

David Romero H. Facultad de Ciencias, Universidad Nacional Autónoma de México. Av. Universidad 3000, UNAM, Coyocán, Ciudad de México, C.P.04510, dromeroh@ciencias.unam.mx

Néstor Corona Morales, Centro de Estudios en Geografía Humana-El Colegio de Michoacán, Cerro de Nahuatzen 85, Fracc. Jardines del Cerro Grande, La Piedad, Mich., México, C.P.59379, corona@colmich.edu.mx

Hector Nava, Dep. de Zoología. Instituto de Investigaciones sobre los Recursos Naturales. Universidad Michoacana de San Nicolás de Hidalgo. Av. San Juanito Itzícuaro S/N, Nueva Esperanza, Morelia Mich. México., C.P.58337, hector.nava@umich.mx

Hamblet Torija Morales, H. Cuerpo de Bomberos Oaxaca- Blvrd. Chahue 1 sector H2, 70980 Santa Cruz Huatulco, Oaxaca, Mx, hamblettorija@gmail.com

Felipe Hernández Maguey, Instituto de Geofísica, UNAM, Circuito de la Investigación Científica s/n, Ciudad Universitaria, Coyoacán, C.P.04510, Ciudad de México, fhmaguey@igeofisica.unam.mx

List of Figure Captions

Figure 1. Tectonic and earthquake setting. Red bullseye – Mw> 7 earthquakes in the Oaxaca region (SSM, 2020b); star – 23 June 2020 epicenter (SSM, 2020a); Moment tensor of the 23 June 2020 earthquake (USGS (2020).

Figure 2. Vertical zonation of the organisms used in this study.

Figure 3. Coseismic uplift generated by the La Crucecita Mw 7.4, 23 June 2020, earthquake. Bars indicate the width (m) of the organisms bleached belt (OBB) at 15 locations along 44 km of coastal stretch: 1. San Isidro, 2. Playa del Amor, 3. San Agustín, 4. Bahía Riscalillo, 5. Playa el Órgano, 6. Playa el Violín, 7. Playa Yerbabuena – SEMAR, 8. Playa Pescadores, 9. Fonatur dock, 10. Marina Chahué, 11. Playa Pescadores – Quinta Real, 12. La Bocana Río Copalita, 13. Río Zimatán, 14. Zimatán – Laguna las Garzas, 15. Barra de la Cruz. Blue triangles – sites with values > 0.5 m. Please see the text for explanation.

Figure 4. Mortality of intertidal organisms caused by sudden land uplift shown by a bleaching belt of intertidal organisms. UL = Upper limit and LL Lower limit of organism bleached belt. a) La Bocana Río Copalita , b) San Isidro, c) Bahía Riscalillo – aerial view of patches of

bleached coral reef, d) Marina Chahué, e) Playa el Violín,   f) Bleached coral reef at Bahía Riscalillo g) Playa Yerbabuena – SEMAR – bleached coral, h) Playa Pescadores, i). Detail of bleached belt at Playa Pescadores.

Figure 5. Tsunami runup marked by debris at four locations along the study area. a) El Violín Beach, b) Marina Chahué, c) Playa Yerbabuena – SEMAR.

Figure 6. Other Geologic effects: liquefaction, fissures, landslides caused by La crucecita earthquake of 23 June 2020. a) Playa Pescadores – Quinta Real, b), c) y g) Zimatán-Laguna las Garzas, d) La Bocana Río Copalita, e), f) Boulevar Chahué.

Figure 7. Surveying during COVID-19 crisis. A) Arrival at Huatulco airport and reception by the Bomberos de Oaxaca (Oaxaca Firemen). b) SEMAR (Mexican Navy) vessel used to reach inaccessible by land coastal locations. c) Instructions and discussion with SEMAR members keeping a safe distance and wearing masks. d) Sign at Barra de La Cruz indicating restricted access to the town due to COVID-19 confinement.

Supplemental material

Date	Local Hour	Date (UTC)	Hour (UTC)	Elevation (m) (measured from zero Tide Gauge)	Elevation (m) (measured from Mean Sea Level)
25.06.2020	14.45	25.06.2020	19:45	2.112	-0.213
25.06.2020	14.50	25.06.2020	19:50	2.148	-0.177
25.06.2020	15.22	25.06.2020	20:22	2.313	-0.012
25.06.2020	16.32	25.06.2020	21:32	2.670	0.345
25.06.2020	16.39	25.06.2020	21:39	2.680	0.355
25.06.2020	19.47	26.06.2020	00:47	2.870	0.545
25.06.2020	19.56	26.06.2020	00:56	2.880	0.555
25.06.2020	19.57	26.06.2020	00:57	2.880	0.555
26.06.2020	08.20	26.06.2020	13:20	2.690	0.365
26.06.2020	08.25	26.06.2020	13:25	2.660	0.335
26.06.2020	08.28	26.06.2020	13:28	2.650	0.325
26.06.2020	15.15	26.06.2020	20:15	2.090	-0.235
26.06.2020	15.16	26.06.2020	20:16	2.090	-0.235
26.06.2020	15.18	26.06.2020	20:18	2.080	-0.245
26.06.2020	15.47	26.06.2020	20:47	2.200	-0.125
26.06.2020	16.50	26.06.2020	21:50	2.460	0.135
26.06.2020	17.01	26.06.2020	22:01	2.630	0.305
26.06.2020	17.13	26.06.2020	22:13	2.650	0.325
26.06.2020	17.16	26.06.2020	22:16	2.680	0.355
26.06.2020	17.30	26.06.2020	22:13	2.650	0.325
26.06.2020	18.30	26.06.2020	23:30	2.845	0.52

27.06.2020	11.11	27.06.2020	16:11	2.410	0.085
27.06.2020	11.18	27.06.2020	16:18	2.329	0.004
27.06.2020	11.24	27.06.2020	16:24	2.300	-0.025
27.06.2020	11.28	27.06.2020	16:28	2.300	-0.025
27.06.2020	11.41	27.06.2020	16:41	2.2300	-0.095
27.06.2020	12.28	27.06.2020	17:28	2.160	-0.165
27.06.2020	13.45	27.06.2020	18:45	1.950	-0.375
27.06.2020	14.05	27.06.2020	19:05	1.980	-0.345
27.06.2020	14.36	27.06.2020	19:36	1.890	-0.435
27.06.2020	16.15	27.06.2020	21:15	2.110	-0.215
27.06.2020	20.30	28.06.2020	01:30	2.08	1.037
27.06.2020	21.00	28.06.2020	02:00	2.049	1.006
28.06.2020	10.57	28.06.2020	15:57	1.840	0.797
28.06.2020	11.32	28.06.2020	16:32	1.718	0.675
28.06.2020	11.34	28.06.2020	16:34	1.711	0.668
28.06.2020	12.27	28.06.2020	17:27	1.516	0.473
28.06.2020	12.31	28.06.2020	17:31	1.501	0.458
28.06.2020	12.45	28.06.2020	17:45	1.452	0.409
28.06.2020	13.37	28.06.2020	18:37	1.292	0.249
28.06.2020	13.55	28.06.2020	18:55	1.249	0.206
28.06.2020	16.12	28.06.2020	21:12	1.251	0.208
28.06.2020	18.12	28.06.2020	23:12	1.624	0.581

Table S1. Tide gauge data from Servicio Mareográfico Nacional (SMN) at Huatulco station. Data were used to assess living position and mortality of intertidal organisms.

Table S2. Taxonomic identity and vertical zonation of organisms used in this study.

Taxa	Gastropod mollusk	Algae	Barnacle	Barnacle	Polychaete	Bivalve mollusk
Kingdom	Animalia	Plantae	Animalia	Animalia	Animalia	Animalia
Subkingdom	-	Viridiplantae	-	-	-	-
Phyllum	Mollusca	Chlorophyta	Arthropoda	Arthropoda	Annelida	Mollusca
Subphyllum	-	Chlorophytina	Crustacea	Crustacea	-	-
Superclass	-		Multicrustacea	Multicrustacea	-	-
Class	Gastropoda	Ulvophyceae	Hexanauplia	Hexanauplia	Polychaeta	Bivalvia
Subclass	Neritimorpha		Thecostraca	Thecostraca	Sedentaria	Autobranchia
Infraclass	-		Cirripedia	Cirripedia	Canalipalpata	Pteriomorphia
Subterclass	-		-	-	-	-
Superorder	-		Thoacica	Thoacica	-	-
Order	Cycloneritida	Ulvales	Sessilia	Sessilia	Sabellida	Ostreida
Suborder			Balanomorpha	Balanomorpha	-	-
Superfamily	Neritoidea		Balanoidea	Balanoidea	-	Ostreoidea
Family	Neritidae	Ulvaceae	Balanidae	Balanidae	Serpulidae	Ostreidae
Subfamily	Neritinae		Megabalaninae	Amphibalaninae	-	Crassostreinae
Tribe			-	-	-	-
Genus	*Nerita*	*Ulva*	*Megabalanus*	*Amphibalanus*	Salmacina	*Crassostrea*
Species	*Nerita scabricosta* Lamarck, 1822	*Ulva prolifera* O.F.Müller, 1778	*Megabalanus coccopoma* (Darwin, 1854)	*Amphibalanus eburneus* (Gould, 1841)	*Salmacina tribranchiata* (Moore, 1923)	*Crassostrea corteziensis* (Hertlein, 1951)
Vertical zonation	Subtidal and intertidal species, this mollusk growths on hard substrata from above the limit of the highest tides.	Intertidal species, this algae growths from the upper limit of the high tides.	Intertidal species, this barnacle inhabits hard substrata from the upper limit of the high tides up to 100 m depth.	Intertidal species, this barnacle inhabits hard substrata from the upper limit of the high tides.	Intertidal species, this polychaete inhabits hard substrata from the upper limit of the high tides up to 116 m depth.	Intertidal and subtidal species, this mollusk inhabits hard substrata from the upper limit of the high tides.

Table S2 (continuation). Taxonomic identity and vertical zonation of organisms used in this study.

Taxa	Bivalve mollusk	Bivalve mollusk	Gastropod mollusk	Vermetid mollusk	Coralline algae	Stony coral	Stony coral
Kingdom	Animalia	Animalia	Animalia	Animalia	Plantae	Animalia	Animalia
Subkingdom	-	-	-	-	Biliphyta	-	-
Phyllum	Mollusca	Mollusca	Mollusca	Mollusca	Rhodophyta	Cnidaria	Cnidaria
Subphyllum	-	-	-	-	Eurhodophytina	-	-
Superclass	-	-	-	-	-	-	-
Class	Bivalvia	Bivalvia	Gastropoda	Gastropoda	Florideophyceae	Anthozoa	Anthozoa
Subclass	Autobranchia	Autobranchia	Patellogastropoda	Caenogastropoda	Corallinophycidae	Hexacorallia	Hexacorallia
Infraclass	Pteriomorphia	Heteroconchia	-		-	-	-
Subterclass	-	Euheterodonta	-		-	-	-
Superorder	-	Imparidentia	-		-	-	-
Order	Ostreida	Venerida	-	Littorinimorpha	Corallinales	Scleractinia	Scleractinia
Suborder	-		-		-	-	-
Superfamily	Ostreoidea	Chamoidea	Lottioidea	Vermetoidea	-	-	-
Family	Ostreidae	Chamidae	Lottiidae	Vermetidae	Lithophyllaceae	Pocilloporidae	Pocilloporidae
Subfamily	Saccostreinae		Lottiinae		Lithophylloideae	-	-
Tribe	-		Lottiini		Lithophylleae	-	-
Genus	*Saccostrea*	*Chama*	*Lottia*	*Petaloconchus*	*Lithophyllum*	*Pocillopora*	*Pocillopora*
Species	*Saccostrea palmula* (Carpenter, 1857)	*Chama coralloides Reeve, 1846*	*Lottia pediculus* (Philippi, 1846)	*Petaloconchus complicatus* Dall, 1908	Lithophyllum sp.	*Pocillopora verrucosa* (Ellis & Solander, 1786)	*Pocillopora damicornis* (Linnaeus, 1758)
Vertical zonation	Intertidal and subtidal species, this mollusk inhabits hard substrata from the upper limit of the high tides.	Intertidal and subtidal species, this mollusk inhabits hard substrata from the upper limit of the high tides.	Intertidal and subtidal species, this mollusk inhabits hard substrata from the upper limit of the high tides.	Intertidal and subtidal species, this mollusk inhabits hard substrata from the upper limit of the high tides.	Subtidal species, this algae growths permanently submerged on hard substrata below the lower limit of the low tides.	Subtidal species, this colonize hard substrata below the lowest limit of the low tide up to 30 m depth.	Subtidal species, this colonize hard substrata below the lowest limit of the low tide up to 30 m depth.

Table S2. Taxonomic identity and vertical zonation of organisms used in this study.

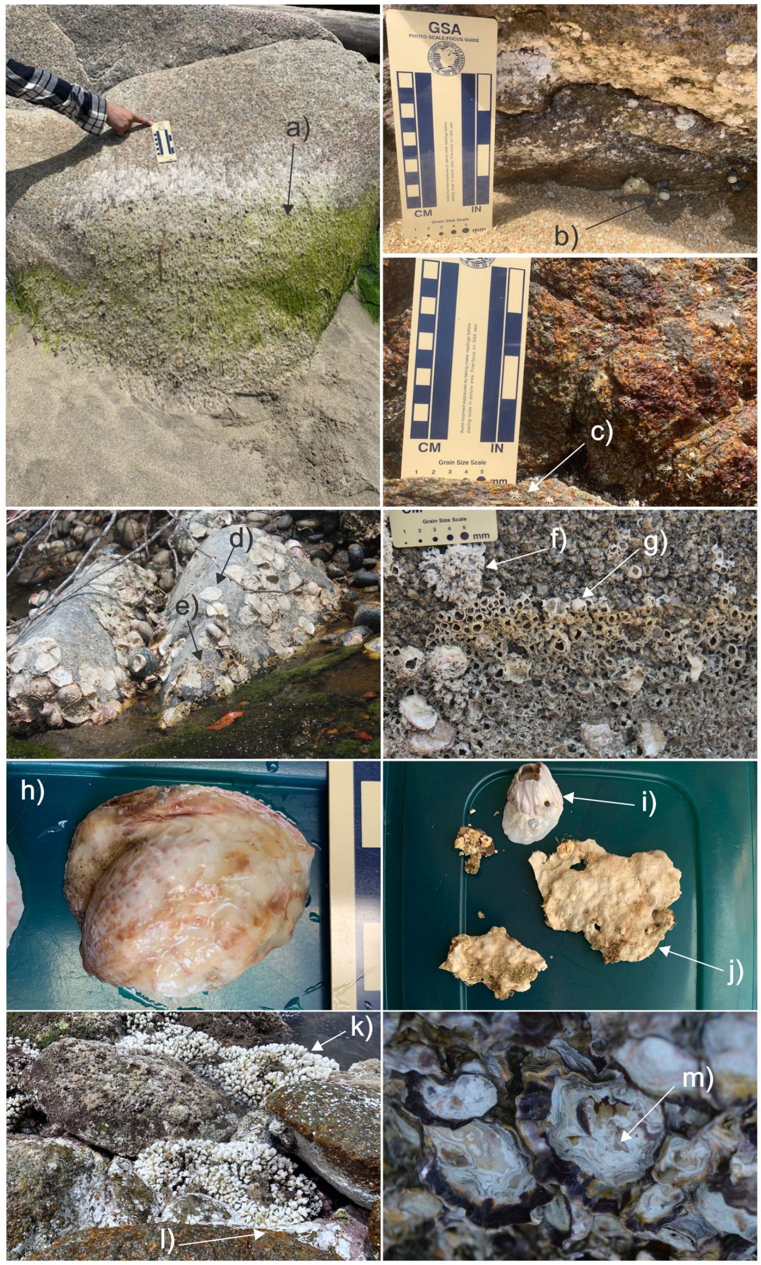

Figure S1. Detail of biomarkers used in this study: a) algae *Ulva prolifera*, b) gastropod *Nerita scabricosta*, c) gastropod *Lottia pediculus*, d) bivalve *Crassostrea corteziensis*, e) vermetid *Petaloconchus complicatus*, f) polychaete *Salmacina tribranchiata*, g) crustacean *Amphibalanus eburneus*, h) bivalve *Chama coralloides*, i) crustacean *Megabalanus coccopoma,* j) coralline algae *Lithophyllum* sp., k) stony coral *Pocillopora verrucosa* and l) stony coral *Pocillopora damicornis*, m) bivalve *Saccostrea palmula*.

Figure S1. Detail of organisms used in this study: a) algae Ulva prolifera, b) gastropod Nerita scabricosta, c) gastropod Lottia pediculus, d) bivalve Crassostrea corteziensis, e) vermetid Petaloconchus complicatus, f) polychaete Salmacina tribranchiata, g) crustacean Amphibalanus eburneus, h) bivalve Chama coralloides, i) crustacean Megabalanus coccopoma, j) coralline algae Lithophyllum sp., k) stony coral Pocillopora verrucosa and l) stony coral Pocillopora damicornis, m) Saccostrea palmula.

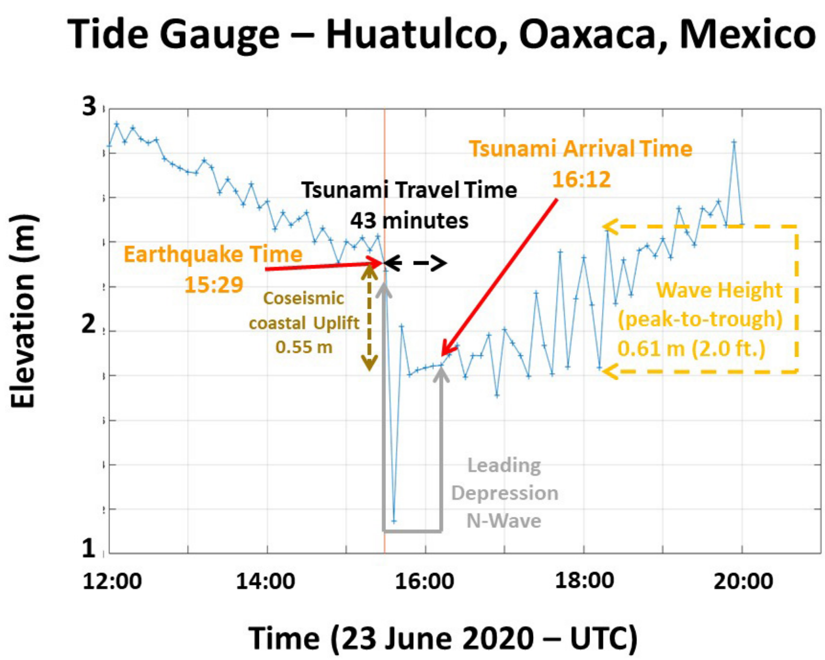

Figure S2. Huatulco tide gauge data interpretation of land level vertical displacement and tsunami amplitude after the 23 June

Figure S2. Huatulco tide gauge data interpretation of land level vertical displacement and tsunami amplitude after the 23 June 2020 earthquake.